PdCu single atom alloys for the selective oxidation of methanol to methyl formate at low temperatures

Junjun Shan[1,2,*], Georgios Giannakakis[1], Jilei Liu[1], Sufeng Cao[1], Ouyang Mengyao[1], Mengwei Li[1], Sungsik Lee[3], Maria Flytzani-Stephanopoulos[1]

[1]*Department of Chemical and Biological Engineering, Tufts University, Medford MA, 02155*

[2]*NICE America Research, Inc., Mountain View, CA, 94043*

[3]*X-ray Science Division, Argonne National Laboratory, 9700 South Cass Avenue, Lemont, IL 60439*

**corresponding author: Junjun.Shan@nicenergy.com*

Abstract

The selective catalytic oxidation of methanol to methyl formate (MF) has been considered as an attractive route to produce MF, an important precursor in the chemical industry. Although supported Pd nanoparticles are active for the selective oxidation of methanol to MF, the relative low MF selectivity and yield remains an unsolved issue. Herein, we show that adding a small amount of Pd into Cu forming PdCu single atom alloy (SAA) catalysts can catalyze the oxidation of methanol to MF selectively at low temperatures, with a high catalyst stability. The atomic dispersion of Pd atoms in the Cu matrix was confirmed by various in-situ characterization techniques. The activity and selectivity of PdCu SAA catalysts were compared to monometallic Cu and Pd catalysts, in a flow reactor at similar conditions. This work may guide the design of new SAA based catalysts for selective oxidation reactions.

Introduction

Methyl formate (MF) is an important chemical intermediate for the synthesis of various valuable industrial products such as carboxylic acids, ethylene glycol, and formamides [1-4]. Currently, MF is produced commercially by the carbonylation of methanol with carbon monoxide, catalyzed by strong liquid bases for example sodium methoxide [4-6]. However, the deactivation of the catalyst and undesirable side-products caused by some impurities in the reagents remain as major challenges of this process [1, 4, 7]. Therefore, it is highly attractive to develop new process to produce MF with high selectivity and long catalyst lifetime. The selective oxidation of methanol at low temperatures has been considered as an attractive green route to produce MF [3, 7-10].

A wide array of catalysts have been studied for methanol oxidation to MF, including various metal oxides [3, 11-16], and supported noble metal nanoparticles (NPs) [7, 17-22], among latter, supported Pd based NPs has attracted significant attentions [7, 10, 17, 19-22]. It has been found that even monometallic Pd NPs are active in methanol oxidation to MF [17, 21, 22]. For example, Wojcieszak et al. reported that a methanol conversion of ~67% with a MF selectivity of ~82% can be achieved at 80 °C over Pd/TiO_2 catalysts [21]. J. G. Wang and co-authors found that silica supported Au-Pd bimetallic nanoparticles can achieve MF selectivity of ~73% with a methanol conversion of ~57% at 130 °C [22]. However, in all these studies, MF can only be produced at low temperatures with relatively low yield. At slightly high temperatures (> 130 °C), the over-oxidation to CO_2 dominates on these Pd based catalysts. Furthermore, a relatively high Pd loading is needed for Pd based catalysts (typically 1-2 wt%), indicating a low utilization of Pd atoms. Naturally, it is highly desirable to develop new Pd based catalysts to increase noble metal utilization and reduce CO_2 selectivity.

In addition, it has also been reported that unsupported gold, prepared in nanoporous form from AuAg alloys after leaching out most of the silver, is an effective catalyst for the selective oxidation of methanol to MF [2, 23, 24]. As unsupported gold itself is inert, the active sites must be at the interface of silver

domains and gold, suggesting that the majority gold atoms do not participate in the reaction. Similar to supported Pd nanoparticles, the low utilization of gold atoms is a major disadvantage of unsupported nanoporous AuAg catalysts.

To increase noble metal utilization, the design of atomically dispersed supported metal catalysts on various supports has attracted tremendous attention in recent years [25-27]. Extending to metal matrices, novel single atom alloy (SAA) catalysts that are composed of singly dispersed active metal atoms embedded into a less active host metal, have been synthesized and reported to exhibit unique catalytic performance for a variety of hydrogenation and dehydrogenation reactions [28-36]. For example, PdCu SAA catalysts exhibit an order of magnitude higher activity for the phenylacetylene hydrogenation compared to monometallic Cu, while maintaining a high selectivity to styrene [28]. PtCu SAA catalysts are highly active and selective for 1,3 butadiene hydrogenation to butene under mild conditions [30]. PdAu SAA catalysts show high activity towards the selective hydrogenation of 1-hexyne to 1-hexene at low temperatures [33]. NiCu SAA catalysts can catalyze the non-oxidative dehydrogenation of ethanol, selectively to acetaldehyde and hydrogen products by facilitating the C-H bond cleavage [35]. The unique catalytic activities of these SAA catalysts in various hydrogenation and dehydrogenation reactions are attributed to the presence of isolated active metal atoms that act as entrance and exit routes for hydrogen dissociation and re-combination. Spillover of H atoms onto the Cu surfaces contributes to the increased activity in hydrogenation reactions.

In the present study, we examined the catalytic activity of PdCu SAA catalysts in the selective methanol oxidation reaction. PdCu SAA catalysts were prepared through the galvanic replacement method. The atomic dispersion of Pd atoms in Cu matrices was confirmed through various characterization techniques. The prepared PdCu SAA catalysts show high activity, selectivity, and catalyst stability towards the selective oxidation of methanol to MF. In addition, we compared the performance of PdCu SAA catalysts with monometallic Cu, monometallic Pd catalysts. Our data show a remarkable promotional effect for PdCu SAA catalysts.

Experimental

Catalyst preparation

Silica supported PdCu SAAs were prepared by the galvanic replacement method, as was described in our previous publications [29, 35]. Here, we give a brief overview of the procedure. In the first step, metallic Cu nanoparticles were prepared as colloids in solution. According, under nitrogen protection, a 0.1 M solution of ascorbic acid was added to a mixed aqueous solution of $Cu(NO_3)_2$ and polyvinylpyrrolidone (PVP) (200:1 molar ratio of Cu to PVP), followed by drop-wise addition of $NaBH_4$ (0.1 M), upon which the solution turned to an opaque brown suspension. Fumed silica, with a surface area of 200 m^2/g (as received), was pre-activated by heating in air at 650 °C for 12 h, suspended in deionized water under constant stirring, and added drop-wise to the colloidal solution. The solution was kept under nitrogen protection and constant stirring for 30 min, followed by filtering and washing with deionized water several times. The collected solid was dried in vacuum for 12 h and calcined in air to 350 ^oC for 4 h. The product was subsequently reduced in pure hydrogen at 350 °C for 3h to obtain silica supported metallic Cu NPs. The typical Cu loading is 8 wt%, as was determined by inductively coupled plasma (ICP) elemental analysis.

The galvanic replacement (GR) method was used to deposit Pd atoms into the Cu surface. The addition of Pd atoms to Cu NPs was performed in an aqueous solution at room temperature with nitrogen protection and continuous stirring. Desired amounts of $Pd(NO_3)_2 \cdot 6H_2O$ were added to a suspension of Cu NPs at room temperature. The reaction was held for 1h under nitrogen protection and constant stirring, and then the solid was filtered and washed with deionized water several times. The obtained product was dried in vacuum at 60 ^oC overnight, and was reduced in hydrogen (10% balanced in He) at 350 °C for 1h to obtain silica supported PdCu SAA NPs catalysts. The typical atomic ratio of Pd to Cu ranges from 1:10 to 1:100, as was measured by ICP.

Characterization methods

X-ray powder diffraction (XRD) patterns were collected on a PANalytical X'Pert Pro instrument using nickel-filtered Cu Kα radiation (λ = 1.54056 Å). The measurements were taken at 45 kV and 40 mA in a continuous mode. Data was collected for 2θ between 25° and 80°. ICP was performed with a Leeman Labs PS1000 instrument. High resolution transmission electron microscopy (HR-TEM) was conducted on a JEOL 2010 electron microscope. The specimens were obtained by drying one drop of ethanol solution of NPs onto a carbon film with copper covered microgrid. UV-Vis absorption spectra were collected in the range of 200 - 800 nm using a Jasco V570 UV-Vis Spectrophotometer.

Diffuse reflectance infrared Fourier transform spectroscopy (DRIFTS) measurements were conducted on a Thermo Scientific Nicolet iS50 FTIR Spectrometer and a Praying Mantis high temperature reaction chamber. Typically, samples were reduced *in situ* with 10% H_2/He at a flow rate of 10mL/min at 350°C for 1 h before measurements. CO adsorption on the PdCu SAA samples was performed at room temperature. Pure CO was introduced into the DRIFTS cell at a flow rate of 10 mL/min. This was followed by a He purge at a flow rate of 20 mL/min to remove gas phase CO in the cell prior to DRIFTS measurements.

In-situ X-ray Absorption Near Edge Structure (XANES), and Extended X-Ray Absorption Fine Structure (EXAFS) measurements were performed at beamline 12-BM at Argonne National Laboratory. XANES and EXAFS data of PdCu SAA samples at the Pd K-edge in fluorescence mode were collected. XANES and EXAFS data of Pd metal foil were also collected in the reference mode for X-ray energy calibration and data alignment. Approximately 7 consecutive scans were collected for each sample to improve the signal-to-noise ratio. EXAFS data processing and analysis were performed using the IFEFFIT package.

The selective methanol oxidation activities of PdCu SAA catalysts were evaluated in a fixed-bed flow reactor at atmospheric pressure. Certain amounts of catalysts were loaded into a quartz reactor tube between two layers of quartz sand and packed in between two quartz wool plugs. The reactor was heated in a furnace equipped with a temperature controller. The temperature of the catalyst was measured with a K-type thermocouple reaching the top of the catalyst bed. Prior to testing, all catalysts were reduced under a flow

of H_2 (10% in argon) with a flow rate of 10 mL/min at 350 °C for 1 h. Methanol was introduced into the reactor through a bubbler system with He flow. The reaction gas composition was 10 % methanol and 10% oxygen balanced in He, with a total flow rate of 20 mL/min. The effluent gas was monitored online by a residual gas analyzer (SRS RGA 200) and Gas chromatography (GC).

Results and discussion

The GR procedure was applied to add Pd atoms into the surface of Cu NPs. Ultraviolet-visible spectroscopy (UV-Vis) was used to verify the uptake of Pd atoms during the process. Figure 1 shows UV-Vis spectra of the GR filtrates after replacement of Cu with Pd and the solution of the Pd^{2+} standard. A strong absorption band at 270 nm is present in the spectrum of the Pd^{2+} standard, which is consistent with literatures [37]. In contrast to the Pd^{2+} standard, the GR wash solution did not show any absorption band at 270 nm, suggesting the fully update of Pd atoms during the GR procedure.

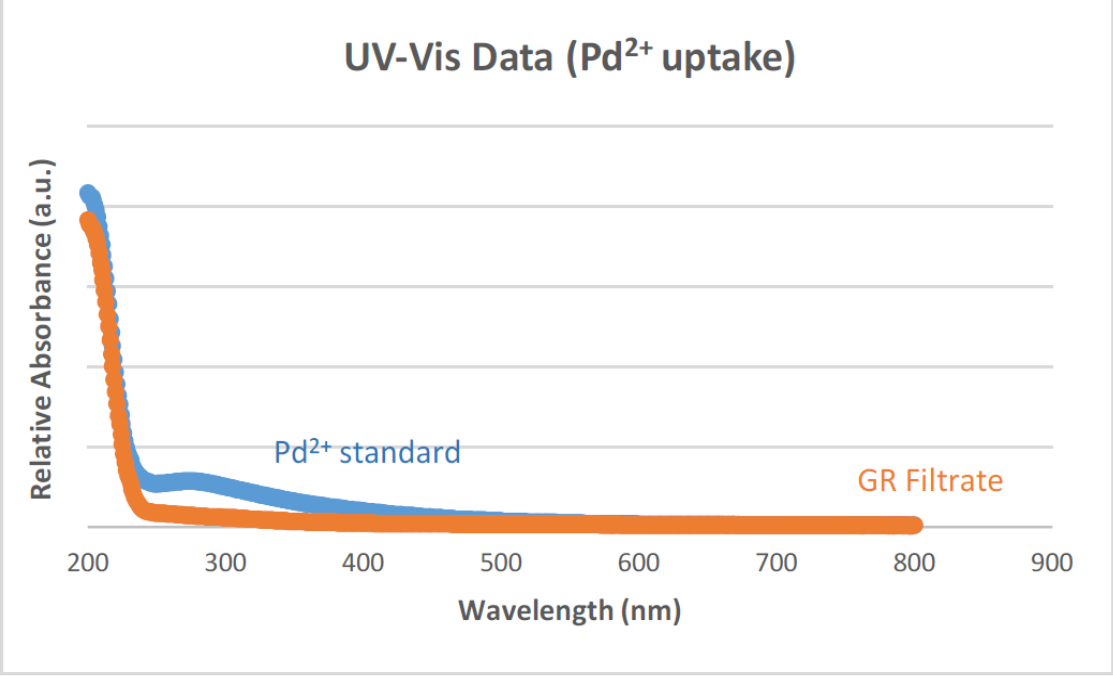

Figure 1, UV-Vis spectra of Pd^{2+} standards compared to the filtrate from GR preparation of PdCu SAA catalysts.

Figure 2 shows the XRD patterns of silica supported Cu NPs after *ex-situ* reduction (bottom trace), silica supported $Pd_{0.01}Cu$ SAA NPs after *ex-situ* reduction (middle trace), and silica supported $Pd_{0.01}Cu$ SAA NPs after selective methanol oxidation reaction and reduction (top trace). The XRD pattern of the supported Cu NPs shows metallic Cu diffraction peaks, (111), (200) and (220) [38]. A small and broad peak centered at 37° can be attributed to the (111) diffraction of a small amount of Cu_2O [34]. XRD patterns of silica-supported $Pd_{0.01}Cu$ SAA NPs show no observable difference as compared to Cu NPs, indicating that introduction of small amounts of Pd through GR does not change the lattice structure of the Cu NPs. Moreover, the XRD pattern of supported $Pd_{0.01}Cu$ SAA NPs after the reaction is preserved, suggesting that selective methanol oxidation reaction does not alter the lattice structure of Cu, and does not oxidize Cu NPs to Cu oxide NPs.

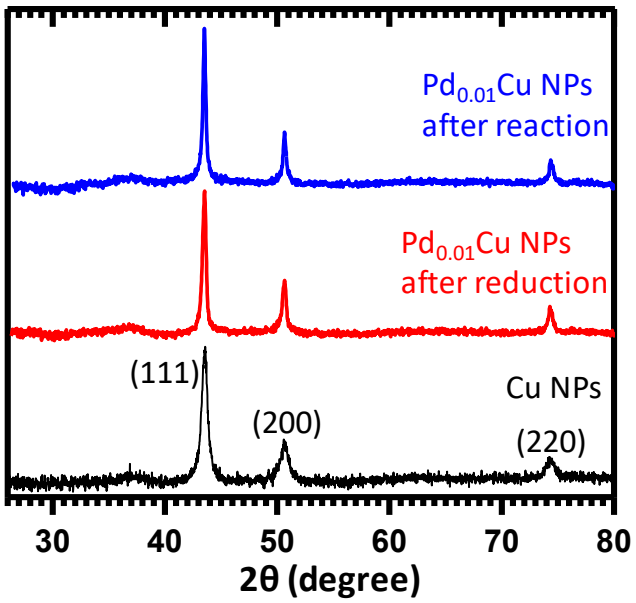

Figure 2, XRD patterns of silica supported Cu NPs after ex-situ reduction (bottom trace), silica supported $Pd_{0.01}Cu$ SAA NPs after ex-situ reduction (middle trace), and silica supported $Pd_{0.01}Cu$ SAA NPs after selective methanol oxidation reaction and reduction (top trace).

Figure 3a and 3b shows the HRTEM images of silica supported $Pd_{0.01}Cu$ SAA catalysts. The sample was first pre-reduced in H_2 atmosphere at 350 °C before TEM measurements. HRTEM images of $Pd_{0.01}Cu$ SAA samples show that average particle size ranges from 6 nm to 14 nm.

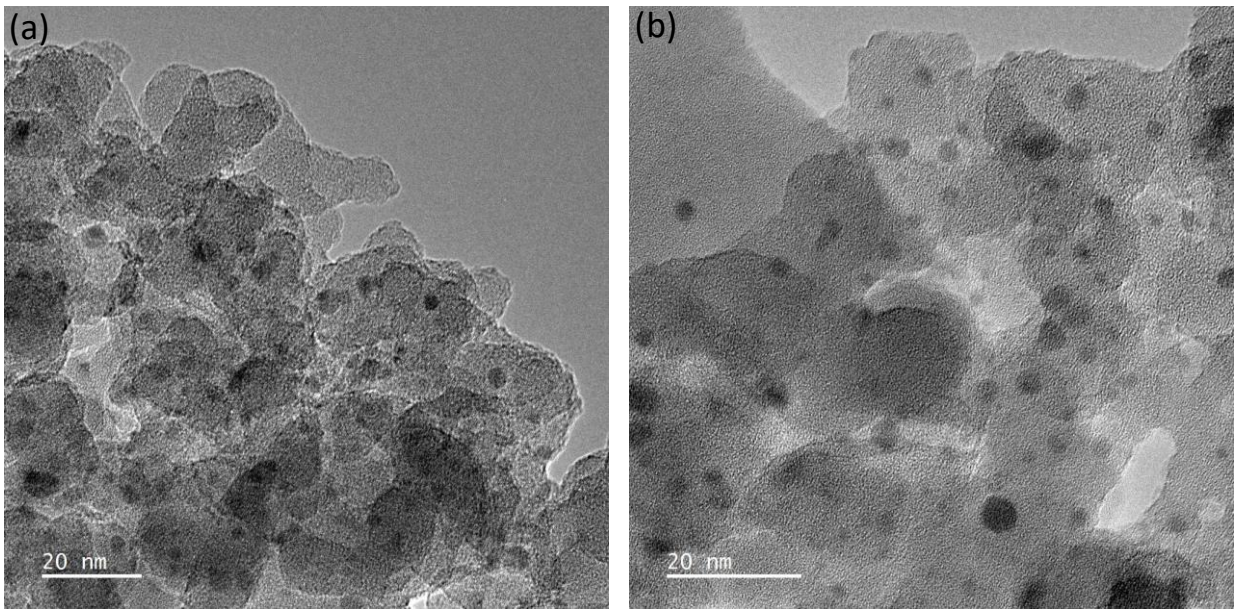

Figure 3, HRTEM images of silica supported $Pd_{0.01}Cu$ SAA catalysts after *ex-situ* reduction.

As shown in Figure 4, using CO as a probe molecule, DRIFTS measurements were performed on Cu NPs, $Pd_{0.01}Cu$ NPs, and Pd NPs. All samples were reduced *in situ* in 10% H_2 (balanced in Ar) at 350 °C for 1h prior to the introduction of CO. The adsorption of CO was performed at room temperature with a flow rate of 10 mL/min followed by a He purge at a flow rate of 20 mL/min for 10 min. CO-DRIFT spectra of Cu NPs show a single peak centered at approximately 2128 cm^{-1}, which can be attributed to either the Cu^{+}-CO carbonyl species or the atop binding of CO on Cu NPs [34, 39]. On the other hand, two adsorption peaks on Pd NPs are present, centered at 1937 cm^{-1} and 2033 cm^{-1}, respectively. Based on literatures, the peak at 1937 cm^{-1} corresponds to bridge adsorbed CO on the extended Pd surface of metallic Pd NPs, whereas, the peak at 2033 cm^{-1} is related to atop binding of CO on Pd atoms [33]. On the other hand, for $Pd_{0.01}Cu$ NPs, only the peaks at 2128 cm^{-1} and 2033 cm^{-1} are present, indicating atop CO adsorption on Cu

NPs and Pd atoms, but no bridge adsorption of CO on Pd NPs. This observation suggests that for $Pd_{0.01}Cu$ NPs, Pd atoms are fully singly dispersed in Cu matrix, forming PdCu SAA catalyst.

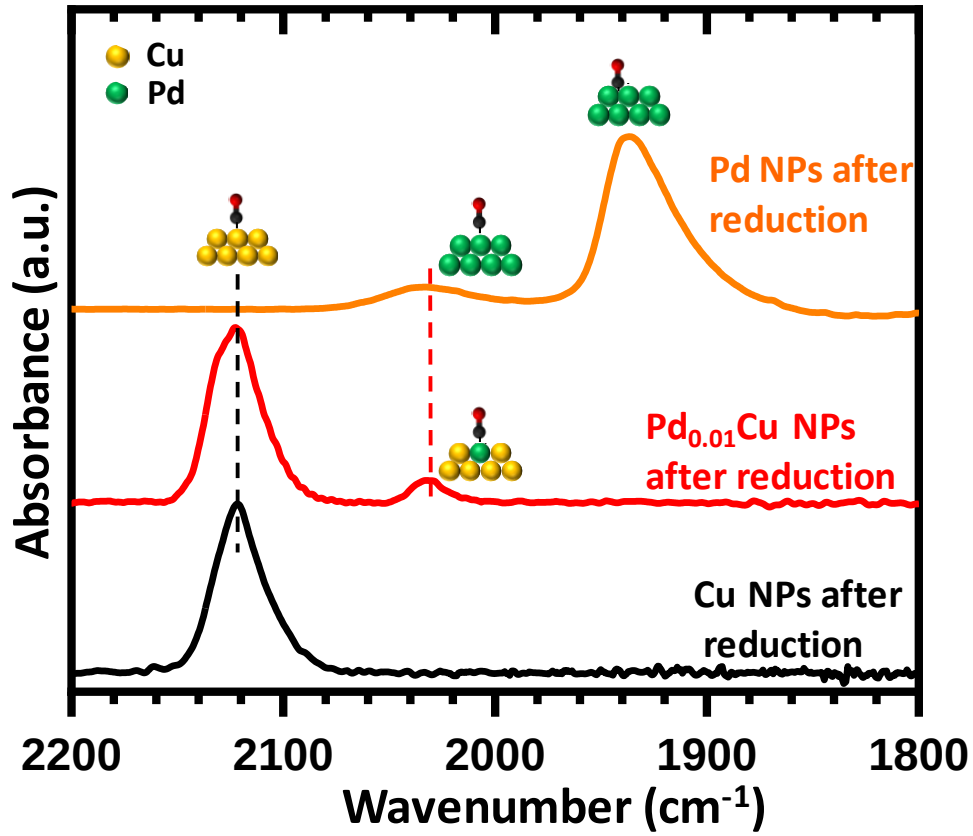

Figure 4, CO-DRIFT spectra of supported Cu NPs, $Pd_{0.01}Cu$ NPs, and Pd NPs. All samples were reduced *in situ* at 350 °C in hydrogen (10% balanced in Ar) for 1h. The CO adsorption was performed at room temperature with a flow rate of 10 mL/min followed by a He purge with a flow rate of 20 mL/min for 10 min prior to DRIFTS measurements.

Figure 5 shows Pd K-edge X-ray Absorption Spectroscopy (XAS) data of $Pd_{0.01}Cu$ NPs after reduction and after methanol oxidation reaction, as well as PdO and Pd foil standards. Figure 5a shows XANES spectra, while Figure 5b shows EXAFS data. XAS data of PdCu SAA samples were collected in fluorescence mode, while the data of Pd standards were collected in the transmission mode. For the data of PdCu SAAs after reduction, sample were *in-situ* reduced in 4% H_2 (balanced in N_2) at 350 °C for 1h and cooled down to room temperature in N_2 atmosphere, prior to collecting XAS data. Whereas, for the data of

PdCu after reaction, samples were treated with 10 % methanol and 10% oxygen at 150 °C for 1h, followed by N_2 purge at room temperature.

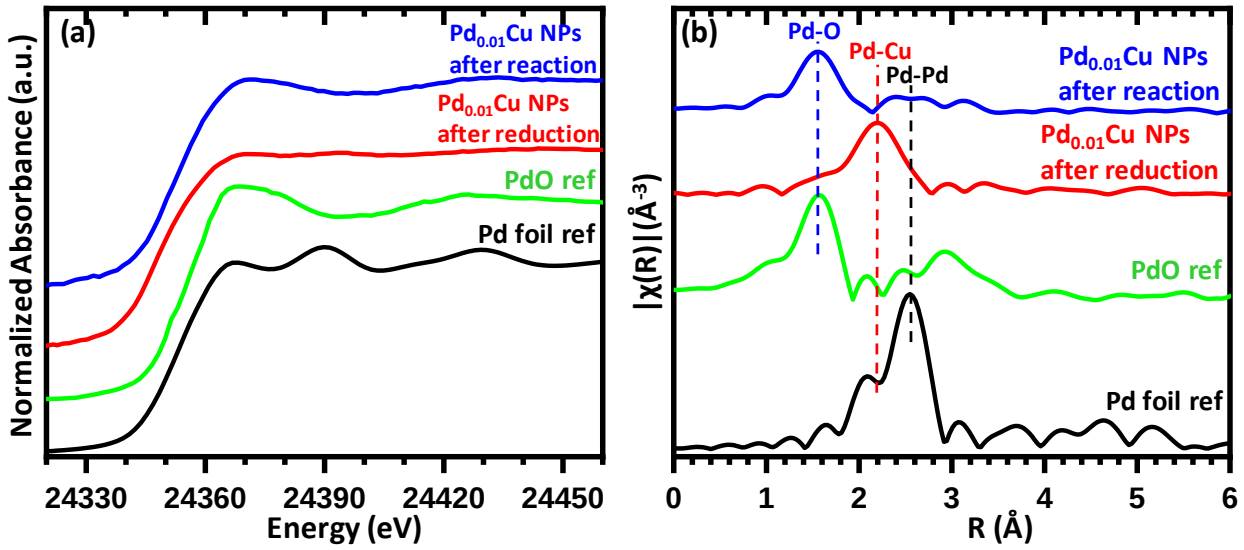

Figure 5a and 5b, in-situ XANES (5a) and EXAFS (5b) data of $Pd_{0.01}Cu$ NPs after reduction and after methanol oxidation reaction, as well as PdO and Pd foil standards. In the case of PdCu NPs, data were collected at fluorescence mode, while the data of Pd standards were collected in the transmission mode.

The XANES spectrum of $Pd_{0.01}Cu$ SAA NPs in Figure 5a clearly shows that after reduction, Pd is not in 2+ oxidation state. Interestingly, the spectrum also does not resemble metallic Pd foil. Indeed, similar Pd K-edge spectra have been reported on PdCu bimetallic alloys in literatures [40, 41]. Thus, our XANES data of $Pd_{0.01}Cu$ NPs suggest that after reduction, Pd atoms are alloyed with Cu atoms, forming bimetallic SAA catalysts, which is consistent with our CO-DFIFTS data in Figure 4. On the other hand, for $Pd_{0.01}Cu$ NPs after reaction, Pd XANES spectrum is similar to PdO reference, indicating that Pd is in 2+ oxidation state after methanol oxidation reaction.

The details of Pd binding environment of $Pd_{0.01}Cu$ NPs were described through the Pd K-edge EXAFS data in R-space as shown in Figure 5b. The EXAFS data of Pd foil and PdO references demonstrate that Pd K-edge peak in R-space of Pd-Pd bonds locates at 2.5 Å, while the peak of Pd-O bonds is at 1.6 Å, in a good agreement with the literature [40]. For $Pd_{0.01}Cu$ NPs after reduction, a new peak centered at 2.2 Å

appears, indicating different binding environment of Pd atoms in $Pd_{0.01}Cu$ NPs comparing to Pd atoms in PdO and metallic foil reference. It has been reported that for bimetallic PdCu alloys, Pd K-edge EXAFS peak in R-space is located at 2.2 Å, and this peak was attributed to Pd-Cu interactions [40, 41]. Therefore, we also assign the peak at 2.2 Å in the case of $Pd_{0.01}Cu$ NPs after reduction to the scattering interaction between Pd atoms and Cu atoms. The lack of peak associated with Pd-Pd interaction at 2.5 Å also suggests that majority Pd atoms in $Pd_{0.01}Cu$ NPs are singly dispersed and alloyed with Cu atoms. This conclusion is in-line with our CO-DRIFTS and XANES results. In addition, EXAFS data of $Pd_{0.01}Cu$ NPs after reaction also show that the peak at 1.6 Å dominates, suggesting the formation of Pd-O bonds after methanol oxidation reaction, in a good agreement with XANES data. In addition, EXAFS data also show that after selective methanol oxidation reaction, there is no formation of Pd-Pd bonds. Thus, it is likely that isolated Pd atoms were oxidized to isolated Pd cations.

As discussed above, our characterization data demonstrate that the prepared supported $Pd_{0.01}Cu$ NPs form SAA NPs, in other words Pd atoms are singly dispersed in the surface of Cu NPs. Such PdCu SAA catalysts were examined with selective methanol oxidation reaction under ambient pressure, and their performance were presented in Figure 6, Figure 7, Figure 8, and Table 1.

Figure 6a shows the temperature-programmed surface reaction (TPSR) data of methanol (10% balanced in He) and oxygen (10% balanced in He) on silica supported Cu NPs, whereas Figure 6b shows TPSR data on silica supported $Pd_{0.01}Cu$ NPs. TPSR data were performed with a heating rate of 5 °C/min in the temperature range from 25 °C to 200 °C at ambient pressure. TPSR data on Cu NPs show that in the temperature below 160 °C, there is no increase of the RGA signal of MF. At the temperature above 160 °C, there is a very small increase of the RGA signal of MF, however the RGA signal of CO_2 also increase. Figure 6a thus demonstrates that Cu NPs is not active for the selective methanol oxidation to MF.

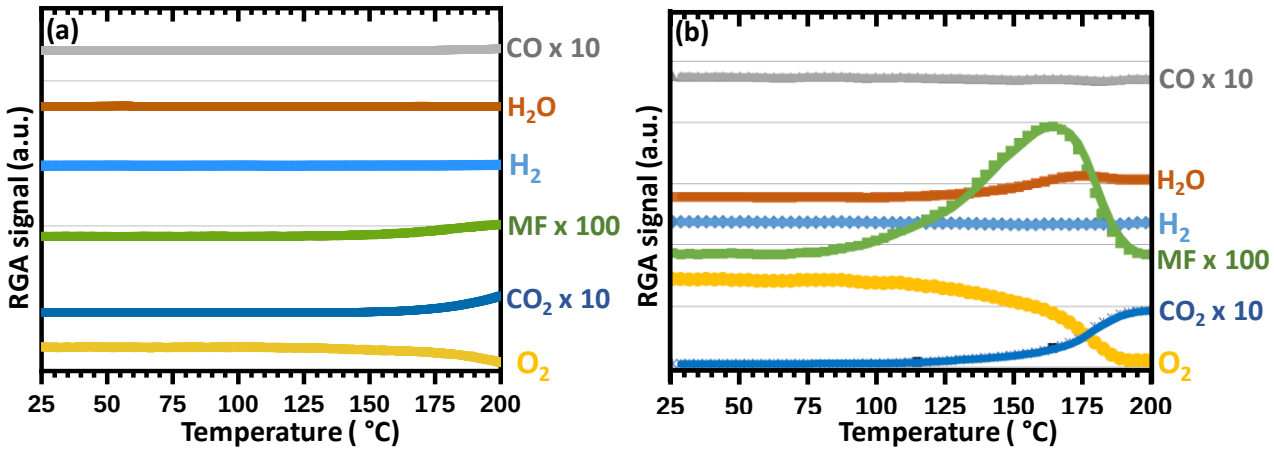

Figure 6a and 6b, TPSR data of methanol (10% balanced in He) and oxygen (10% balanced in He) on silica supported Cu NPs (6a) and silica supported $Pd_{0.01}Cu$ NPs (6b).

On the other hand, TPSR data on $Pd_{0.01}Cu$ NPs in Figure 6b clearly show the formation of MF even at the temperature as low as 90 °C. The formation of MF reaches maximum at the temperature at approximate 160 °C. Apparently, $Pd_{0.01}Cu$ NPs are much more active than Cu NPs in the selective methanol oxidation to MF. Furthermore, Figure 6b also shows that in the temperature below 160 °C, MF is the dominant product, whereas above 160 °C, the formation of CO_2 significantly increases and the formation of MF decreases.

The performance of Cu NPs and $Pd_{0.01}Cu$ NPs in selective methanol oxidation reaction were also examined under steady state conditions. Figure 7 shows the catalytic performance of these catalysts in term of MF yield in the temperature range of 25 °C to 200 °C. In agreement with TPSR data, Figure 7 clearly shows that there is barely any activity on silica supported Cu NPs for selective methanol oxidation to MF. Whereas, on silica supported $Pd_{0.01}Cu$ NPs, the light-off temperature is as low as 90 °C. The maximum MF yield on $Pd_{0.01}Cu$ NPs can reach ~60% at the temperature of 160 °C. Above 160 °C, MF yield decreases, because of the increase of CO_2 selectivity.

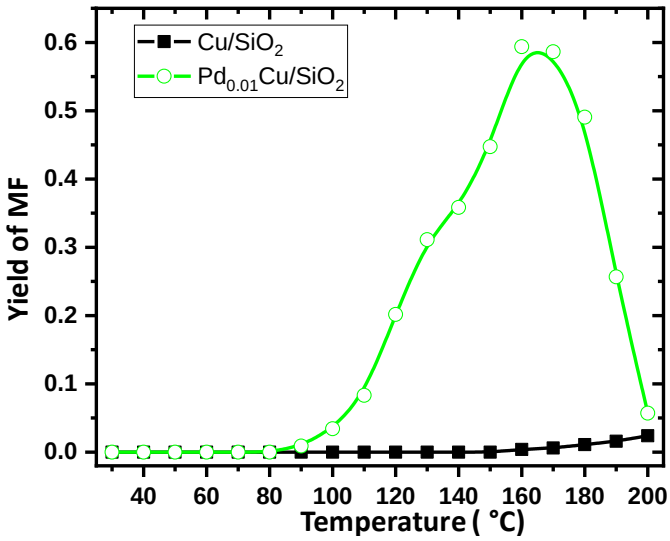

Figure 7, the performance of Cu NPs and $Pd_{0.01}Cu$ NPs in term of MF yield in selective methanol oxidation reaction.

In addition, Table 1 lists methanol conversion, MF selectivity, CO_2 selectivity, and MF yield of Cu NPs and $Pd_{0.01}Cu$ NPs, as well as silica supported Pd NPs with Pd loading at 0.2wt% in selective methanol oxidation reaction at 100 °C, 130 °C, and 160 °C. As agreed with Figure 6 and 7, table 1 also shows that silica supported Cu NPs is not active for selective methanol oxidation. Although silica supported Pd NPs do show some activity, MF selectivity and yield are relatively low. For example, the maximum MF yield that can be achieved on Pd NPs is only at ~24% with MF selectivity at ~58%, when the reaction temperature is at 130 °C. Similar performance on silica supported Pd NPs has been reported before in literatures [21, 22]. Whereas, for $Pd_{0.01}Cu$ NPs at 130 °C, our data show that MF selectivity is at ~97% and MF yield is at ~31%. The maximum MF yield that can be achieved is at ~60% with MF selectivity at 92%, when the reaction temperature is at 160 °C.

Table 1, methanol conversion, MF selectivity, CO_2 selectivity, and MF yield of silica supported Cu NPs, $Pd_{0.01}Cu$ NPs, and Pd NPs in selective methanol oxidation reaction at 100 °C, 130 °C, and 160 °C.

Catalyst	Temperature (°C)	Methanol conversion (%)	MF Selectivity (%)	CO_2 Selectivity (%)	MF yield (%)
Cu/SiO_2	100	0	N/A	N/A	N/A
	130	0	N/A	N/A	N/A
	160	1	50	50	0.5
Pd/SiO_2	100	9.7	88.1	11.9	8.5
	130	35.2	58.3	41.7	24.3
	160	100	0	100	0
$Pd_{0.01}Cu/SiO_2$	100	3.5	99	1	3.5
	130	32.0	97	3	31.1
	160	65.3	92	9	60.1

Fig. 8 shows long-term stability tests of $Pd_{0.01}Cu$ NPs in selective methanol oxidation reaction at 130 °C for approximately 10 h. Both methanol conversion and MF selectivity show no noticeable decrease after the reaction for 10 h. Clearly, $Pd_{0.01}Cu$ SAA catalysts exhibit high stability in selective methanol oxidation reaction. The high stability also indicates that there is no change of the isolation nature of Pd species, in other words, there is no formation of aggregated Pd patches. This observation is also consistent with our characterization results.

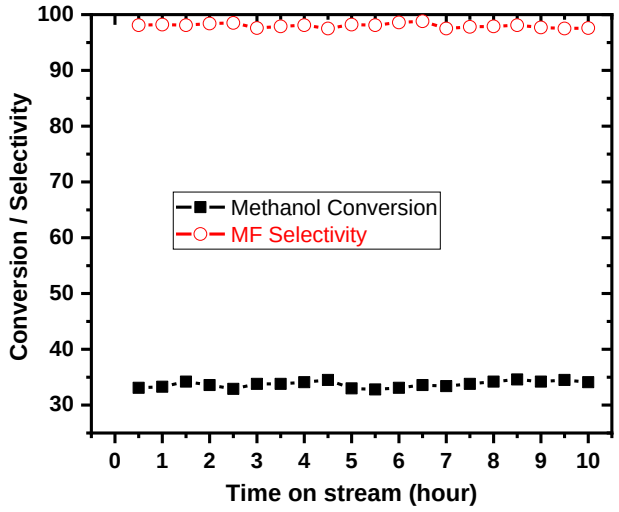

Figure 8, long-term stability of $Pd_{0.01}Cu$ NPs in selective methanol oxidation reaction at 130 °C for approximately 10 h.

Our catalytic measurements clearly demonstrated that supported Cu NPs is not active for selective methanol oxidation to MF. Although supported Pd NPs is active, the low MF selectivity and yield as well as low Pd metal utilization suggests that supported Pd NPs is not an ideal catalyst for this reaction. Interestingly, adding isolated Pd atoms to Cu forming PdCu SAA NPs can significantly increase the activity and MF selectivity, as well as maximum MF yield. PdCu SAA catalysts also exhibit high catalyst stability in selective methanol oxidation reaction.

It has been demonstrated before that isolated active metal atoms embedded in Cu activate and dissociate hydrogen, and the H atoms spilling over onto the bare Cu surface where they are weakly bound and effective for hydrogenation reactions [30, 33]. Moreover, isolated Pt and Ni atoms in Cu can also significantly lower the barrier for C-H bond activation, therefore exhibit improved activity in dehydrogenation reactions [35, 36]. Surprisingly, there are much less SAA studies reported on oxidation reactions. Lucci et al. discovered that a PdAu SAA can dramatically alters the desorption temperature of molecular oxygen after oxidation by ozone, and suggested that Pd atoms locally affect oxide formation on the Au surface [42]. In our previous study, we also found that NiAu SAA catalysts are active for the selective oxidation of methacrolein with methanol to methyl methacrylate [43].

In this study, we found that PdCu SAA catalysts exhibits remarkable activity in selective methanol oxidation reaction. Comparing to Cu NPs, the presence of isolated Pd atoms in Cu dramatically enhance the activity of Cu NPs. Whereas, comparing to Pd NPs, PdCu SAA NPs can significantly decrease CO_2 formation, therefore increase maximum MF yield. Our characterization data also show that after selective methanol oxidation reaction, isolated Pd atoms are oxidized to isolated Pd cations, while majority Cu atoms are still in metallic state. Such observation suggest that isolated Pd atoms can be oxidized locally and may also affect oxide formation on the Cu surface. Such atomically dispersed Pd oxide species in Cu surface might be the active sites for selective methanol oxidation reaction with a high selectivity to MF. Likely, PdCu SAA catalysts or other SAA catalysts may also exhibit high activity in other oxidative reactions. Our study thus indeed indicates that bimetallic SAA catalysts could have wide applications in various catalytic reactions other than hydrogenation and dehydrogenation reactions.

Conclusion

In this work, we demonstrated that supported PdCu SAA catalyst are highly active for the selective oxidation of methanol to MF at low temperatures. The presence of isolated Pd atoms in Cu surface not only significantly increase the reactivity, but also improve the MF selectivity and yield. Our data also show that PdCu SAA catalysts have a high catalyst stability in this reaction. Our characterization results also suggest that isolated Pd atoms can be oxidized locally to form atomically dispersed Pd oxide species embedded in the Cu matrix, which is active for selective methanol oxidation. This work opens a new route for the use of bimetallic SAA catalysts for oxidative reactions.

Acknowledgements

This work was supported as part of the Integrated Mesoscale Architectures for Sustainable Catalysis, an Energy Frontier Research Center funded by the U.S. Department of Energy, Office of Science, Basic Energy Sciences under award #DESC0012573. The XAS research used resources of the Advanced Photon

Source, a U.S. Department of Energy (DOE) Office of Science, User Facility operated for the DOE Office of Science by Argonne National Laboratory under Contract No. DE-AC02-06CH11357.

References

[1] Ullmann's Encyclopedia of Industrial Chemistry, Wiley, New York, 2009.
[2] A. Wittstock, V. Zielasek, J. Biener, C.M. Friend, M. Baumer, Nanoporous Gold Catalysts for Selective Gas-Phase Oxidative Coupling of Methanol at Low Temperature, Science, 327 (2010) 319-322.
[3] W. Li, H. Liu, E. Iglesia, Structures and properties of zirconia-supported ruthenium oxide catalysts for the selective oxidation of methanol to methyl formate, J Phys Chem B, 110 (2006) 23337-23342.
[4] J.S. Lee, J.C. Kim, Y.G. Kim, Methyl formate as a new building block in C1 chemistry, Applied Catalysis, 57 (1990) 1-30.
[5] E. Gérard, H. Götz, S. Pellegrini, Y. Castanet, A. Mortreux, Epoxide–tertiary amine combinations as efficient catalysts for methanol carbonylation into methyl formate in the presence of carbon dioxide, Applied Catalysis A: General, 170 (1998) 297-306.
[6] L. He, H. Liu, C.-x. Xiao, Y. Kou, Liquid-phase synthesis of methyl formate via heterogeneous carbonylation of methanol over a soluble copper nanocluster catalyst, Green Chemistry, 10 (2008) 619.
[7] G.T. Whiting, S.A. Kondrat, C. Hammond, N. Dimitratos, Q. He, D.J. Morgan, N.F. Dummer, J.K. Bartley, C.J. Kiely, S.H. Taylor, G.J. Hutchings, Methyl Formate Formation from Methanol Oxidation Using Supported Gold–Palladium Nanoparticles, Acs Catal, 5 (2014) 637-644.
[8] S. Cao, M. Yang, A.O. Elnabawy, A. Trimpalis, S. Li, C. Wang, F. Göltl, Z. Chen, J. Liu, J. Shan, M. Li, T. Haas, K.W. Chapman, S. Lee, L.F. Allard, M. Mavrikakis, M. Flytzani-Stephanopoulos, Single-atom gold oxo-clusters prepared in alkaline solutions catalyse the heterogeneous methanol self-coupling reactions, Nature Chemistry, 11 (2019) 1098-1105.
[9] C. Li, X. Yang, G. Gao, Y. Li, W. Zhang, X. Chen, H. Su, S. Wang, Z. Wang, Copper on the inner surface of mesoporous TiO2 hollow spheres: a highly selective photocatalyst for partial oxidation of methanol to methyl formate, Catal Sci Technol, 9 (2019) 6240-6252.
[10] Q. Zhang, C. Zhu, G. Yang, Y. Sun, D. Wang, J. Liu, High-performance microstructured Au-Ag bimetallic catalyst for oxidative coupling of methanol to methyl formate, Catalysis Communications, 129 (2019) 105741.
[11] H. Yu, K. Zeng, X. Fu, Y. Zhang, F. Peng, H. Wang, J. Yang, RuO2·xH2O Supported on Carbon Nanotubes as a Highly Active Catalyst for Methanol Oxidation, The Journal of Physical Chemistry C, 112 (2008) 11875-11880.
[12] H. Huang, W. Li, H. Liu, Effect of treatment temperature on structures and properties of zirconia-supported ruthenium oxide catalysts for selective oxidation of methanol to methyl formate, Catal Today, 183 (2012) 58-64.
[13] Z. Liu, R. Zhang, S. Wang, N. Li, R. Sima, G. Liu, P. Wu, G. Zeng, S. Li, Y. Sun, Highly Efficient and Stable Vanadia–Titania–Sulfate Catalysts for Methanol Oxidation to Methyl Formate: Synthesis and Mechanistic Study, The Journal of Physical Chemistry C, 120 (2016) 6591-6600.
[14] J. Liu, E. Zhan, W. Cai, J. Li, W. Shen, Methanol Selective Oxidation to Methyl Formate over ReOx/CeO2 Catalysts, Catal Lett, 120 (2007) 274-280.
[15] N. Li, S. Wang, Y. Sun, S. Li, First principles studies on the selectivity of dimethoxymethane and methyl formate in methanol oxidation over V2O5/TiO2-based catalysts, Phys Chem Chem Phys, 19 (2017) 19393-19406.

[16] V.V. Kaichev, G.Y. Popova, Y.A. Chesalov, A.A. Saraev, D.Y. Zemlyanov, S.A. Beloshapkin, A. Knop-Gericke, R. Schlögl, T.V. Andrushkevich, V.I. Bukhtiyarov, Selective oxidation of methanol to form dimethoxymethane and methyl formate over a monolayer V2O5/TiO2 catalyst, J Catal, 311 (2014) 59-70.
[17] R. Wojcieszak, A. Karelovic, E.M. Gaigneaux, P. Ruiz, Oxidation of methanol to methyl formate over supported Pd nanoparticles: insights into the reaction mechanism at low temperature, Catal. Sci. Technol., 4 (2014) 3298-3305.
[18] Z. Yang, J. Li, X. Yang, Y. Wu, Catalytic oxidation of methanol to methyl formate over silver ? a new purpose of a traditional catalysis system, Catal Lett, 100 (2005) 205-211.
[19] C. Han, X. Yang, G. Gao, J. Wang, H. Lu, J. Liu, M. Tong, X. Liang, Selective oxidation of methanol to methyl formate on catalysts of Au–Ag alloy nanoparticles supported on titania under UV irradiation, Green Chem., 16 (2014) 3603-3615.
[20] R. Wang, Z. Wu, C. Chen, Z. Qin, H. Zhu, G. Wang, H. Wang, C. Wu, W. Dong, W. Fan, J. Wang, Graphene-supported Au–Pd bimetallic nanoparticles with excellent catalytic performance in selective oxidation of methanol to methyl formate, Chemical Communications, 49 (2013) 8250.
[21] R. Wojcieszak, E.M. Gaigneaux, P. Ruiz, Direct Methyl Formate Formation from Methanol over Supported Palladium Nanoparticles at Low Temperature, Chemcatchem, 5 (2013) 339-348.
[22] J.-b. Wu, R.-p. Shi, Z.-f. Qin, H. Liu, Z.-k. Li, H.-q. Zhu, Y.-x. Zhao, J.-g. Wang, Selective oxidation of methanol to methyl formate over bimetallic Au-Pd nanoparticles supported on SiO2, Journal of Fuel Chemistry and Technology, 47 (2019) 780-790.
[23] L.-C. Wang, M.L. Personick, S. Karakalos, R. Fushimi, C.M. Friend, R.J. Madix, Active sites for methanol partial oxidation on nanoporous gold catalysts, J Catal, 344 (2016) 778-783.
[24] B. Xu, C.G.F. Siler, R.J. Madix, C.M. Friend, Ag/Au Mixed Sites Promote Oxidative Coupling of Methanol on the Alloy Surface, Chemistry - A European Journal, 20 (2014) 4646-4652.
[25] M. Flytzani-Stephanopoulos, B.C. Gates, Atomically dispersed supported metal catalysts, Annual review of chemical and biomolecular engineering, 3 (2012) 545-574.
[26] X.F. Yang, A.Q. Wang, B.T. Qiao, J. Li, J.Y. Liu, T. Zhang, Single-Atom Catalysts: A New Frontier in Heterogeneous Catalysis, Accounts Chem Res, 46 (2013) 1740-1748.
[27] J.Y. Liu, Catalysis by Supported Single Metal Atoms, Acs Catal, 7 (2017) 34-59.
[28] G. Kyriakou, M.B. Boucher, A.D. Jewell, E.A. Lewis, T.J. Lawton, A.E. Baber, H.L. Tierney, M. Flytzani-Stephanopoulos, E.C.H. Sykes, Isolated Metal Atom Geometries as a Strategy for Selective Heterogeneous Hydrogenations, Science, 335 (2012) 1209-1212.
[29] M.B. Boucher, B. Zugic, G. Cladaras, J. Kammert, M.D. Marcinkowski, T.J. Lawton, E.C.H. Sykes, M. Flytzani-Stephanopoulos, Single atom alloy surface analogs in Pd0.18Cu15 nanoparticles for selective hydrogenation reactions, Phys Chem Chem Phys, 15 (2013) 12187-12196.
[30] F.R. Lucci, J.L. Liu, M.D. Marcinkowski, M. Yang, L.F. Allard, M. Flytzani-Stephanopoulos, E.C.H. Sykes, Selective hydrogenation of 1,3-butadiene on platinum-copper alloys at the single-atom limit, Nat Commun, 6 (2015).
[31] J.L. Liu, F.R. Lucci, M. Yang, S. Lee, M.D. Marcinkowski, A.J. Therrien, C.T. Williams, E.C.H. Sykes, M. Flytzani-Stephanopoulos, Tackling CO Poisoning with Single-Atom Alloy Catalysts, J Am Chem Soc, 138 (2016) 6396-6399.
[32] J. Shan, F.R. Lucci, J. Liu, M. El-Soda, M.D. Marcinkowski, L.F. Allard, E.C.H. Sykes, M. Flytzani-Stephanopoulos, Water co-catalyzed selective dehydrogenation of methanol to formaldehyde and hydrogen, Surface Science, 650 (2016) 121-129.
[33] J. Liu, J. Shan, F.R. Lucci, S. Cao, E.C.H. Sykes, M. Flytzani-Stephanopoulos, Palladium–gold single atom alloy catalysts for liquid phase selective hydrogenation of 1-hexyne, Catal Sci Technol, 7 (2017) 4276-4284.
[34] J. Shan, N. Janvelyan, H. Li, J. Liu, T.M. Egle, J. Ye, M.M. Biener, J. Biener, C.M. Friend, M. Flytzani-Stephanopoulos, Selective non-oxidative dehydrogenation of ethanol to acetaldehyde and hydrogen on highly dilute NiCu alloys, Applied Catalysis B: Environmental, 205 (2017) 541-550.

[35] J. Shan, J. Liu, M. Li, S. Lustig, S. Lee, M. Flytzani-Stephanopoulos, NiCu single atom alloys catalyze the C H bond activation in the selective non- oxidative ethanol dehydrogenation reaction, Applied Catalysis B: Environmental, 226 (2018) 534-543.
[36] M.D. Marcinkowski, M.T. Darby, J. Liu, J.M. Wimble, F.R. Lucci, S. Lee, A. Michaelides, M. Flytzani-Stephanopoulos, M. Stamatakis, E.C.H. Sykes, Pt/Cu single-atom alloys as coke-resistant catalysts for efficient C–H activation, Nature Chemistry, 10 (2018) 325-332.
[37] A. Podborska, M. Wojnicki, Spectroscopic and theoretical analysis of Pd2+−Cl−−H2O system, Journal of Molecular Structure, 1128 (2017) 117-122.
[38] N.A. Dhas, C.P. Raj, A. Gedanken, Synthesis, characterization, and properties of metallic copper nanoparticles, Chem Mater, 10 (1998) 1446-1452.
[39] N.D. Subramanian, C.S.S.R. Kumar, K. Watanabe, P. Fischer, R. Tanaka, J.J. Spivey, A DRIFTS study of CO adsorption and hydrogenation on Cu-based core-shell nanoparticles, Catal Sci Technol, 2 (2012) 621-631.
[40] C. Sarkar, P. Koley, I. Shown, J. Lee, Y.-F. Liao, K. An, J. Tardio, L. Nakka, K.-H. Chen, J. Mondal, Integration of Interfacial and Alloy Effects to Modulate Catalytic Performance of Metal–Organic-Framework-Derived Cu–Pd Nanocrystals toward Hydrogenolysis of 5-Hydroxymethylfurfural, ACS Sustainable Chemistry & Engineering, 7 (2019) 10349-10362.
[41] D.N. Olekszyszen, B.L. Albuquerque, D.d.O. Silva, G.L. Tripodi, D.C. de Oliveira, J.B. Domingos, Core–shell PdCu bimetallic colloidal nanoparticles in Sonogashira cross-coupling reaction: mechanistic insights into the catalyst mode of action, Nanoscale, 12 (2020) 1171-1179.
[42] F.R. Lucci, L. Zhang, T. Thuening, M.B. Uhlman, A.C. Schilling, G. Henkelman, E. Charles H. Sykes, The effect of single pd atoms on the energetics of recombinative O2 desorption from Au(111), Surface Science, 677 (2018) 296-300.
[43] A. Trimpalis, G. Giannakakis, S. Cao, M. Flytzani-Stephanopoulos, NiAu single atom alloys for the selective oxidation of methacrolein with methanol to methyl methacrylate, Catal Today, (2019).